

# CLOSED-LOOP DEEP LEARNING: GENERATING FORWARD MODELS WITH BACK-PROPAGATION

**Sama Daryanavard<sup>1</sup>, Bernd Porr<sup>1</sup>**

<sup>1</sup>Biomedical Engineering Division, School of Engineering, University of Glasgow, Glasgow G12 8QQ, UK.

**Keywords:** Forward models, deep reinforcement learning.

## Abstract

A reflex is a simple closed loop control approach which tries to minimise an error but fails to do so because it will always react too late. An adaptive algorithm can use this error to learn a forward model with the help of predictive cues. For example a driver learns to improve their steering by looking ahead to avoid steering in the last minute. In order to process complex cues such as the road ahead deep learning is a natural choice. However, this is usually only achieved indirectly by employing deep reinforcement learning having a discrete state space. Here, we show how this can be directly achieved by embedding deep learning into a closed loop system and preserving its continuous processing. We show specifically how error back-propagation can be achieved in z-space and in general how gradient based approaches can be analysed in such closed loop scenarios. The performance of this learning paradigm is demonstrated using a line-follower both in simulation and on a real robot that show very fast and continuous learning.

## 1 Introduction

Reinforcement learning [Sutton and Barto, 1998] has enjoyed a revival in recent years, reaching super human levels at video game playing [Guo et al., 2014]. Its success is owed to a combination of variants of Q learning [Watkins and Dayan, 1992] and deep learning [Rumelhart et al., 1986]. This approach is powerful because deep learning is able to map large input spaces, such as camera images or pixels of a video game onto a representation of future rewards or threats which can then inform an actor to create actions as to maximise such future rewards. However, its speed of learning is still slow and its discrete state space limits its applicability to robotics.

Classical control on the other hand operates in continuous time [Phillips, 2000] which potentially offers solutions to the problems encountered in discrete action space.

Adaptive approaches in control develop forward models where an adaptive controller learns to minimise an error arising from a fixed feedback controller (for example Proportional Integral Derivative (PID) controllers) often called “reflex”. This has been shown to work for simple networks [Klopf, 1986, Verschure and Coolen, 1991] where the error signal from the feedback loop successfully learns forward models of simple predictive (reflex-) actions. For example such a network was able to improve the steering actions of a car where a non-optimal hard wired steering is then quickly superseded by a forward model based on camera information of the road ahead. Such learning is close to one shot learning in this scenario because at every time step the error signal from the PID controller is available and adjusts the network [Porr and Wörgötter, 2006]. However, so far these networks could not easily be scaled up to deeper structures and consequently had limited performance [Kulvicius et al., 2007].

A natural step is to employ deep learning [Rumelhart et al., 1986] instead of a shallow network to learn a forward model. If we directly learn a forward model with the deep network mapping sensor inputs to actions then we no longer need a discrete action space. This then will allow to potentially much higher learning rates because the error feedback will be continuous as well. In order to achieve this we need to define a new cost function for our deep network which is defined within the closed loop framework benchmarking the forward model in contrast to a desired output.

In this paper we present a new approach for direct use of deep learning in a closed loop context where it learns to replace a fixed feedback controller with a forward model. We show in an analytical way how to use the Laplace/z-space to solve back-propagation in a closed loop system. We then apply the solution first to a simulated line follower and then to a real robot where a deep network learns fast to replace a simple fixed PID controller with a forward model.

## 2 The learning platform

Before we introduce and explore the deep learner  $N$  we need to establish our closed loop system. The configuration depicted in Fig. 1A) is the architecture of this learning paradigm which provides a closed loop platform for autonomous learning. It consists of an inner reflex loop and an outer predictive loop that contains the learning unit. In the absence of any learning, the reflex loop receives a delayed disturbance  $Dz^{-T}$  via the reflex environment  $Q_R$ ; leads to state  $S_a$ . Given the desired state  $S_d$  the closed loop Error ( $E_c$ ) is generated as:  $E_c = S_d - S_a$ . This drives the agent to take an appropriate reflex action  $A_R$  as to recover to  $S_d$  and force  $E_c$  to zero. However the reflex mechanism  $H_R$  can only react to the disturbance  $D$  after it has perturbed the system.

Hence, the aim of the learning loop is to fend off  $D$  before it has disturbed the state of the robot. To that end, this loop receives  $D$  via the predictive environment  $Q_P$  and in advance of the reflex loop. This provides the learning unit with predictive signals  $P_i$  and, given its internal parameters  $\omega$ , a predictive action is generated as:  $A_P = N(P_i, \omega)$ .

During the learning process,  $A_P$  combined with  $A_R$  and  $Dz^{-T}$  travels through the reflex loop and  $E_c$  is generated. This error signal provides the deep learner  $N$  with a minimal instructive feedback. Upon learning,  $A_P$  fully combats  $D$  on its arrival at the reflex loop (i.e.  $Dz^{-T}$ ); hence the reflex mechanism is no longer evoked and  $E_c$  is kept at zero.

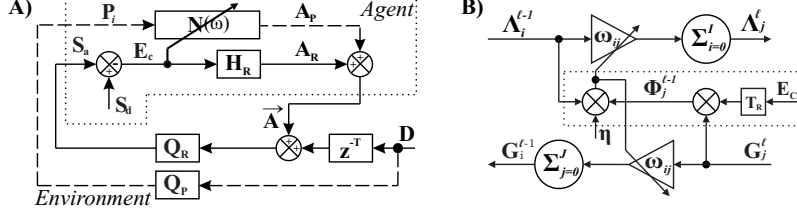


Figure 1: **A)** *The closed loop platform: consists of an inner reflex loop (solid lines) and an outer learning loop (dashed lines), the learning unit  $N(\omega)$  generates a forward model of the environment. Given predictive inputs  $U_i$  (filtered predictive signals  $P_i F_i$ ) it generates an action  $A_P$  that combats the disturbance  $D$  on its arrival at the reflex loop. Finally, the closed loop error  $E_c$  gives an instructive feedback to the learning unit on how well  $A_P$  protected the system from  $D$ .* **B)** *The computational unit: shows the forward and back-propagation of the inputs and the error to the deeper layers. Dotted line marks the correlation of the closed loop error with the internal parameters of the neuron highlighting the update rule, where,  $T_R$  is the transfer function of the reflex loop*

### 3 Closed loop dynamics

The aim of the learning is to keep the closed loop Error  $E_c$  to zero. Referring to Fig. 1A this signal is derived as:  $E_c(z) = S_d(z) - S_a(z)$ ; expansion of  $S_a(z)$  yields:<sup>1</sup>

$$E_c = S_d - Q_R(Dz^{-T} + E_c H_R + A_P) = \frac{S_d - Q_R(Dz^{-T} + A_P)}{1 + H_R Q_R} \quad (1)$$

In mathematical terms, *learning* entails the adjustment of the internal parameters of the learning unit  $\omega$  so that  $E_c$  is kept at zero. To that end, the closed loop Cost-Function  $C_c$  is defined as the square of absolute  $E_c$ :

$$C_c := |E_c|^2 \quad (2)$$

Introduction of closed loop Cost-Function ( $C_c$ ) translates the *learning goal* into adjustments of  $\omega$  so that  $C_c$  is minimised, this in turn ensures that  $E_c$  is kept at zero.

$$\frac{\partial C_c}{\partial \omega} = 2|E_c| \frac{\partial E_c}{\partial \omega} \Big|_{\omega_{min}} = 0 \begin{cases} E_c = 0, \text{ learning goal} \\ E_c \neq 0, \text{ local minima} \end{cases} \quad (3)$$

The behaviour of the gradient  $\frac{\partial C_c}{\partial \omega} = G_\omega^c$  is best explained through separation of gradients of the closed loop and the learner as below:

$$G_\omega^c := \frac{\partial C_c}{\partial \omega} = \frac{\partial C_c}{\partial A_P} \frac{\partial A_P}{\partial \omega} = G_a^{c_c} G_\omega^a \quad (4)$$

The former partial derivative, termed closed loop Gradient  $G_a^{c_c}$ , solely relates to the dynamics of the closed loop platform; this is derived from equations 1 and 2:

$$G_a^{c_c} := \frac{\partial C_c}{\partial A_P} = 2|E_c| \frac{\partial E_c}{\partial A_P} = 2|E_c| \frac{-Q_R}{1 + H_R Q_R} = 2|E_c| T_R \quad (5)$$

Where the resulting fraction  $\frac{-Q_R}{1 + H_R Q_R}$  is the transfer function of the reflex loop  $T_R$ .

<sup>1</sup>For brevity, the complex frequency variable ( $z$ ) will be omitted

## 4 Towards closed loop error backpropagation

To be able to link open loop backpropagation to our closed loop learning paradigm we need to relate our closed loop error  $E_c$  to the standard open loop error of backpropagation. In conventional open-loop implementations, the open-loop Cost-Function  $C_o$  and open-loop Error  $E_o$  are defined at the action output of the network:

$$C_o := |E_o|^2 := |A_P^d - A_P|^2 \quad (6)$$

Where  $A_P^d$  is the desired predictive action. Minimisation of  $C_o$  with respect to the internal parameters of the learning unit  $\omega$  gives:

$$\frac{\partial C_o}{\partial \omega} = \frac{\partial C_o}{\partial A_P} \frac{\partial A_P}{\partial \omega} = G_a^{c_o} G_\omega^a \quad (7)$$

The former partial derivative is termed open-loop Gradient  $G_a^{c_o}$ , from equation 6:

$$G_a^{c_o} = 2E_o \frac{\partial E_o}{\partial A_P} = -2|A_P^d - A_P| \quad (8)$$

Now we relate the open-loop parameters to their closed loop counterparts. Expansion of  $S_d$  in equation 1 gives:

$$E_c = Q_R(Dz^{-T} + E_c H_R + A_P^d) - Q_R(Dz^{-T} + E_c H_R + A_P) = Q_R(A_P^d - A_P) = Q_R E_o \quad (9)$$

Given  $Q_R$  is a non-zero transfer function, the open-loop Error is kept at zero if and only if closed loop Error is kept at zero:

$$Q_R \neq 0 \quad , \text{ therefore: } \quad E_c = 0 \iff E_o = 0 \quad (10)$$

Having now established how the error can be fed into an error backpropagation framework we are now able to present the inner workings of the learning unit.

## 5 The inner workings of the learning unit

Having explored the dynamics of the closed loop, we now focus on the inner working of the learning unit. The latter partial derivative in equations 4 and 7, termed the Network Gradient  $G_\omega^a$ , is merely based on the inner configuration of the learning unit which in this work, is a Deep Neural Network (DNN) with backpropagation (BP). Given that the network is situated in the closed loop platform, its dynamics is expressed in z-space. The Forward-Propagation (FP) entails feeding the predictive inputs  $P_i$  and generating the predictive action  $A_P$ . This is shown in Fig. 1B) with solid line and is expressed as below where  $\Lambda_j^\ell$  denotes the activation of neurons<sup>2</sup>:

$$\Lambda_j^\ell = \sum_{i=0}^I \omega_{ij}^\ell \Lambda_i^{\ell-1} \quad \text{where: } \quad \ell : 0 \rightarrow L \quad \text{note that: } \quad \Lambda_i^{-1} = P_i \quad (11)$$

---

<sup>2</sup>Subscripts refer to the neuron's index and superscripts refer to the layer containing the neuron or weight

$\omega_{ij}^\ell$  denotes the weights of neurons which are analogous to weights in time-domain. Using equation 11,  $G_\omega^a$  with respect to specific weights gives:

$$G_{\omega_{ij}^\ell}^a := \frac{\partial A_P}{\partial \omega_{ij}^\ell} = \frac{\partial A_P}{\partial \Lambda_j^\ell} \frac{\partial \Lambda_j^\ell}{\partial \omega_{ij}^\ell} = \frac{\partial A_P}{\partial \Lambda_j^\ell} \Lambda_i^{\ell-1} \quad (12)$$

The resulting partial derivative is termed Internal Gradient  $G$  and is calculated using backpropagation:

$$G_j^\ell := \frac{\partial A_P}{\partial \Lambda_j^\ell} = \sum_{k=0}^K (w_{jk}^{\ell+1} G_k^{\ell+1}) \quad \text{where: } \ell : L - 1 \rightarrow 0 \quad \text{note that: } G_0^L = 1 \quad (13)$$

Therefore, the Internal Error  $\Phi$  of the neuron, measuring sensitivity of the closed loop Cost-Function with respect to its activation, is given as below; refer to equations 5 and 13:

$$\Phi_j^\ell := \frac{\partial C_c}{\partial \Lambda_j^\ell} = \frac{\partial C_c}{\partial A_P} \frac{\partial A_P}{\partial \Lambda_j^\ell} = 2G_j^\ell |E_c| \frac{-Q_R}{1 + H_R Q_R} \quad (14)$$

The update rule can be expressed as the correlation of the internal error of the neuron with the activation of the previous neuron:

$$\Delta \omega_{ij}^\ell = \eta \Phi_j^\ell(z) \Lambda_i^{\ell-1}(-z) \quad , \quad \eta \ll 1 \quad (15)$$

The small learning rate  $\eta$  ensures that the time-dependant weight change is small. Note that Eq. 15 results in a weight change in the time domain which is calculated in z-space and for that reason we call this learning scheme Inter Domain Learning (IDL).

The gradient of the  $C_c$  with respect to an arbitrary weight is given as following, referring to equations 5, 11, and 14:

$$\frac{\partial C_c}{\partial \omega_{ij}^\ell} = \frac{\partial C_c}{\partial \Lambda_j^\ell} \frac{\partial \Lambda_j^\ell}{\partial \omega_{ij}^\ell} = \frac{-2|E_c|Q_R}{1 + H_R Q_R} \sum_{k=0}^K (w_{jk}^{\ell+1} G_k^{\ell+1}) \Lambda_i^{\ell-1} = \sum_{k=0}^K (w_{jk}^{\ell+1} \Phi_k^{\ell+1}) \Lambda_i^{\ell-1} \quad (16)$$

This shows that the changes in  $C_c$  with respect to an arbitrary weight depends on the weighted internal error introduced in the adjacent deeper layer. This is the propagation of  $C_c$  into the deeper layers and shows the backpropagation in the z-domain.

## 6 Results

The performance of our Inter-Domain Learning (IDL) paradigm is tested using a line-follower both in simulation and through experiments with a real robot. The learning paradigm was developed into a bespoke low-level C++ external library [Dar, 2019]. The transfer function of the reflex loop  $T_R$ , derived in Equation 5, is set to unity for the following results.

## 6.1 Simulations

Fig. 2A shows the configuration of the robot and its environment for simulations. The closed loop error  $E_c$  is calculated using the right and left ground sensors:

$$E_c = G_L - G_R \quad (17)$$

For prediction, 8 predictive signals are generated using an array of 16 ground sensors placed ahead of the robot as shown in the left-hand side of Fig. 2A.

$$P_i = I_j - I_{j^*} \quad , \quad \text{where } j^* \text{ is the sensor index symmetrical to } j \quad (18)$$

These are then filtered using a bank of 5 second-order lowpass filters ( $f_i$ ), with a damping coefficient of  $Q = 0.51$  and impulse responses lasting between 3 to 10 iterations as to cause the correct delay for the correlation of predictors and the error signal. This results in 40 predictive inputs to the network which is configured with 12 and 6 neurons in the first two hidden layers and 1 output neuron in the final layer. The steering of the robot is facilitated through adjustments of the left and right wheel velocities (Fig. 2A):

$$V_R = V_0 + \alpha E_c + \beta \Lambda_0^L \quad , \quad V_L = V_0 - \alpha E_c - \beta \Lambda_0^L \quad \text{and:} \quad \vec{V} = \vec{V}_l + \vec{V}_r \quad (19)$$

Where  $V_0$ ,  $\alpha$  and  $\beta$  are experimental tuning parameters set to  $40 [\frac{m}{s}]$ , 200 and 100 respectively. The simulation environment is shown in Fig. 2B where the robot follows the track from the start point and in a loop for 1000 iterations. A set of simulations were carried out to contrast the reflex and the predictive behaviours; each scenario was repeated 10 times for reproducibility and statistical analysis. Fig. 3A and B show the average closed loop error over 10 trials for reflex and learning ( $\eta = 1e-2$ ) behaviours respectively. A comparison of these results show very fast learning of the robot where the error signal is forced to zero. Top and bottom sections of Fig. 2B show the trajectory of the robot over the course of one trial, for the reflex and learning respectively; in the presence of learning the steering is of anticipatory nature and exhibits a smooth trajectory. Whereas, in the absence of learning the steering is reactive and hence the abrupt response.

Fig. 3D shows the normalised euclidean distance of the weights in each layer from their random initialisation. This shows a gradual increase from zero to its maximum during the course of one simulation. Since the error signal is propagated as a weighted sum of the internal errors all layers show similar rate of change in their weight distance. Moreover, Fig. 3C shows the final distribution of first layer's weights in the form of a normalised greyscale map upon completion of the learning. The weights show an organised distribution, with higher weights associated to the outer predictors,  $P_{2,5}$  and smaller weights associated to the inner predictors,  $P_{4,7,8}$ ; see Fig. 2A for position of predictors. This facilitates a sharper steering for the outer predictors ensuring a smooth trajectory, as shown in the bottom section of Fig. 2B.

Another set of simulations were carried out with five orders of learning rates:  $\eta : \{10^{-5}, 10^{-4}, 10^{-3}, 10^{-2}, 10^{-1}\}$ ; each of the scenarios were repeated 10 times. Fig. 4C shows the Root Mean Square (RMS) of the error signal for each learning trials as well as that of the reflex trials for comparison. All learning scenarios show a significantly smaller RMS error when compared to the reflex behaviour; the error is reduced from over  $8 \cdot 10^{-2}$  to around  $2 \cdot 10^{-2}$  and below. There is a gradual decrease in this value as the learning rate is increased. Smaller values of RMS error indicates both the reduction in the amplitude and also the recurrence of the error signal.

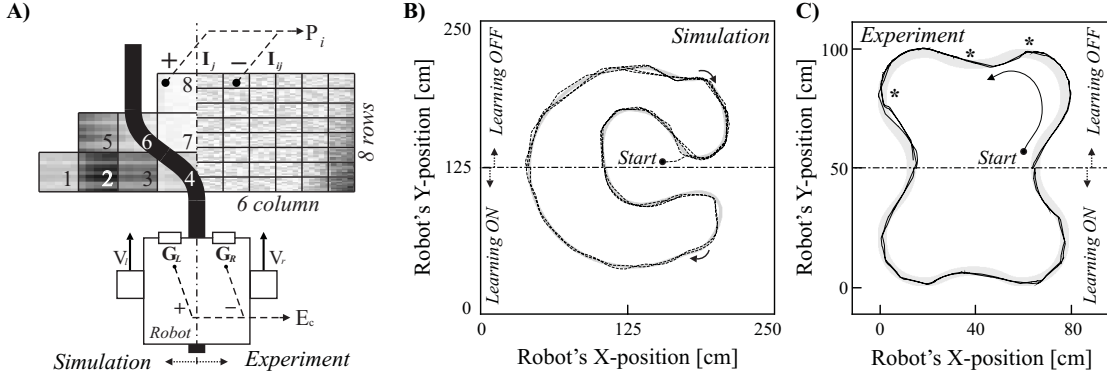


Figure 2: **A)** Schematic of the robot and its environment: the robot is composed of a body with two wheels with speeds of  $V_r$  and  $V_l$  and two ground sensors  $G_r$  and  $G_l$  from which the closed loop error  $E_c$  is generated. The robot is placed on a track and has vision of the path ahead. In simulations this is 16 symmetrical ground sensors (left-hand side) and in real experiments it is the camera view with 6x16 pixels (right-hand side). From this the predictors  $P_i$  are generated as the difference of symmetrical pixels pairs. **B)** and **C)** The Track and robot's trajectory for simulations and experiments respectively. In both cases the top section shows the trajectory of the robot during a reflex trial showing a poor uneven trace whereas the bottom section shows the trajectory for a learning trial showing a smooth and even trace.

## 6.2 Experiments

The experiments with a real robot were carried out using a Parallax SumoBot as a mechanical test-bed, a Raspberry Pi 3B+ for computation and an Arduino Nano as the motor controller. For predictive learning a camera was mounted on the robot providing vision of the path ahead (see right-hand side of Fig. 2) as a matrix of pixels,  $[I]_{NM}$ , from which the predictive signals  $P_{ij}$  are extracted :

$$P_{ij} = I_{ij} - I_{ij^*} \quad , \text{ where } j^* \text{ is the sensor index symmetrical to } j \quad (20)$$

With 6 columns and 8 rows, 48 predictive signals were extracted and filtered using 5 second-order low-pass filters with  $Q = 0.51$  and impulse responses lasting from 5 to 10 time steps to cause the correct delay. The error signal was defined as a weighted sum of 3 light sensors for a smoother and more informative error signal. The deep neural network was configured with 11 hidden layers each with 11 neurons, as well as an output layer with 3 neurons to facilitate slow, medium and sharp steering.

Fig. 5A Shows the closed-loop error in the absence of learning. This is when the robot navigates using its reflex system only. It can be seen that the error signal is very persistent in this case as the robot can only generate an appropriate steering command retrospectively after an error has occurred. This sets a benchmark for evaluation of the deep learner. Fig. 5B shows the error signal in the presence of the deep learner where the learning rate is  $\eta = 2 \cdot 10^{-1}$ , this shows a strong reduction of the error signal over the first 1500 steps, where the learning is achieved rapidly using the closed-loop error that acts as a minimal instructive feedback for the deep learner. Fig. 5C shows the final distribution of the weights in the first layer associating different strength to different pixel location of the predictors. From the gradient it can be seen that the farther the

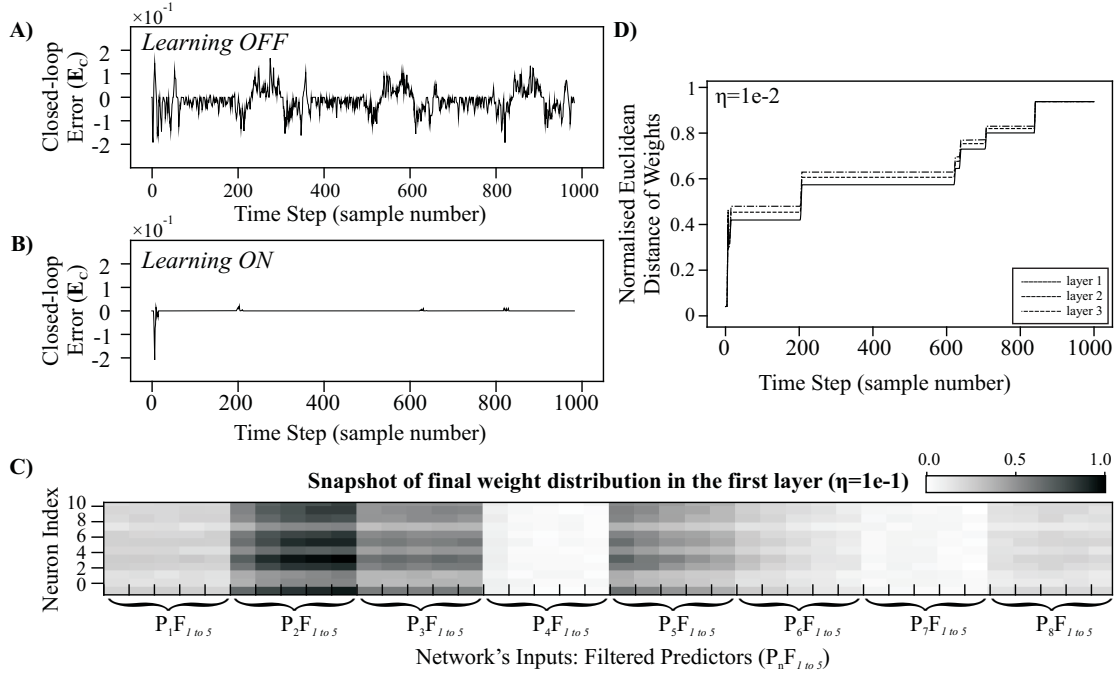


Figure 3: *Simulation results: A) Shows robot’s closed-loop error signal when navigating by reflex mechanism only, note the high amplitude ( $RMS=0.05$ ) and frequent occurrence of the error whilst the learning is off. B) Shows robot’s closed-loop error signal when navigating by reflex mechanism and learning ( $\eta = 10^{-2}$ ) mechanism, note that both the amplitude ( $RMS=0.01$ ) and the occurrence of the error has reduced significantly with learning compared to that of reflex only. C) Shows greyscale map of the weight distribution in the first layer after the learning is completed ( $\eta = 10^{-2}$ ). Note that the weight distribution closely follow the location of predictors to which they associate, with weights associated to outermost predictors having high values and weights associated to innermost predictors having small values to allow for abrupt and subtle steering of the robot respectively. For position of predictors refer to Fig. 2A. D) Shows normalised euclidean distance of the weights in each layer during learning ( $\eta = 10^{-2}$ ), note the gradual increase of the weight distance that stabilises towards the end of learning where the error is kept at zero.*

predictor from the centre line the greater the steering action, this is also illustrated in Fig. 2A. Fig. 5D shows the weight change in each layer as explained in the simulation results. The weight distance changes noticeably over the first 1500 steps dictated by the closed-loop error but comes to a stable plateau as the error signal remains at zero.

Fig. 2C shows the robot’s track and compares the trajectory of the robot for a reflex and a learning trial. Top section of the figure shows that when the learning is off the trace of robot almost always remains outside of the track with a few crossover points indicated by a star. Whereas, the bottom section shows that with learning ( $\eta = 2.10^{-1}$ ) the trace of robot is aligned with the track.

The performance of the deep learner ( $\eta = 2 \cdot 10^{-1}$ ) was repeated with 5 different random weight initialisation using different random seeds  $srand(i)$  where  $i = \{0, 1, 2, 3, 4\}$ . In the presence of learning, ”success” refers to a condition where the closed-loop error shows a minimum of 75 percent reduction from its average value dur-



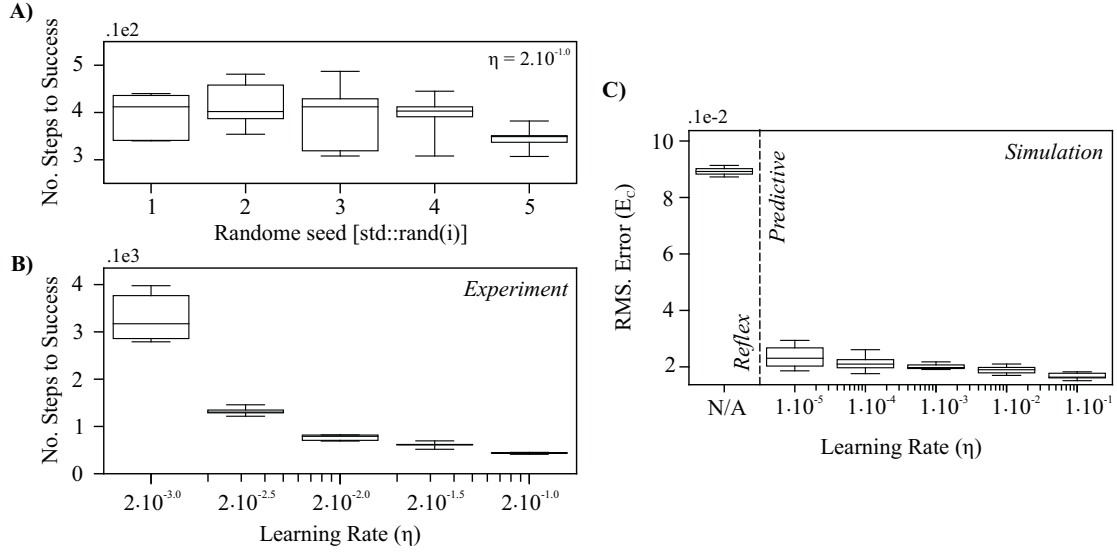


Figure 4: **A)** Shows the number of steps taken until the success condition is met for 5 different random seed for weight initialisation. Note that the random initialisation of weights plays no significant role in the learning and success time. **B)** Shows the effect of learning rate on the number of step taken until the success condition is met. Data shows a significant exponential decrease in the time taken before a successful learning is achieved. In other words, the learning is significantly faster for higher learning rates as it varies from  $2.10^{-3}$  to  $2.10^{-1}$ . **C)** Shows the effect of learning rate on RMS value of closed-loop error  $E_c$ . Note the significant reduction of the closed-loop error in the presence of learning compared to that of reflex only, as well as the gradual improvement of learning (faster learning) with exponential increase of the learning rate  $\eta$  from  $10^{-5}$  to  $10^{-1}$ . Examples of these trials are shown in Fig. 3A and B for reflex and learning with  $\eta = 10^{-2}$  respectively.

ing reflex only trials, for 100 consequent steps. Fig. 4A shows that different random initialisation of the weights makes no significant difference to the time that it takes for the learner to meet the success condition.

The experiment was repeated with a 5 different learning rates  $\eta : \{2.10^{-3}, 2.10^{-2.5}, 2.10^{-2}, 2.10^{-1.5}, 2.10^{-1}\}$ ; each experiment was repeated 5 times for reproducibility. Fig. 4B shows the time taken to success for these trials. This data shows an exponential decay of the success time as the learning rate is increased.

Fig. 6 shows another example of a learning trial similar to that in Fig. 5 but with a smaller learning rate  $\eta = 2.10^{-3}$ . Fig. 6A shows the contribution of the deep learner to the resultant differential speed of the robot. This quantity is small and inaccurate at the start of the trial where the reflex mechanism governs the navigation of the robot, however, the contribution of the learner grows larger and more precise over time as the learner begins to dominate the navigation. This transition from reflex to learning navigation is also seen in Fig. 6B where the error signal  $E_c$  decreases gradually as a successful learning is approached. Fig. 5C shows the final distribution of the weights in the first layer and shows similar but more crude gradients compared to that of Fig. 6C. Fig. 5D shows the weight change in each layer during learning. This shows a more gradual change compared to the learning trial with  $\eta = 2.10^{-1}$  shown in Fig. 5D.

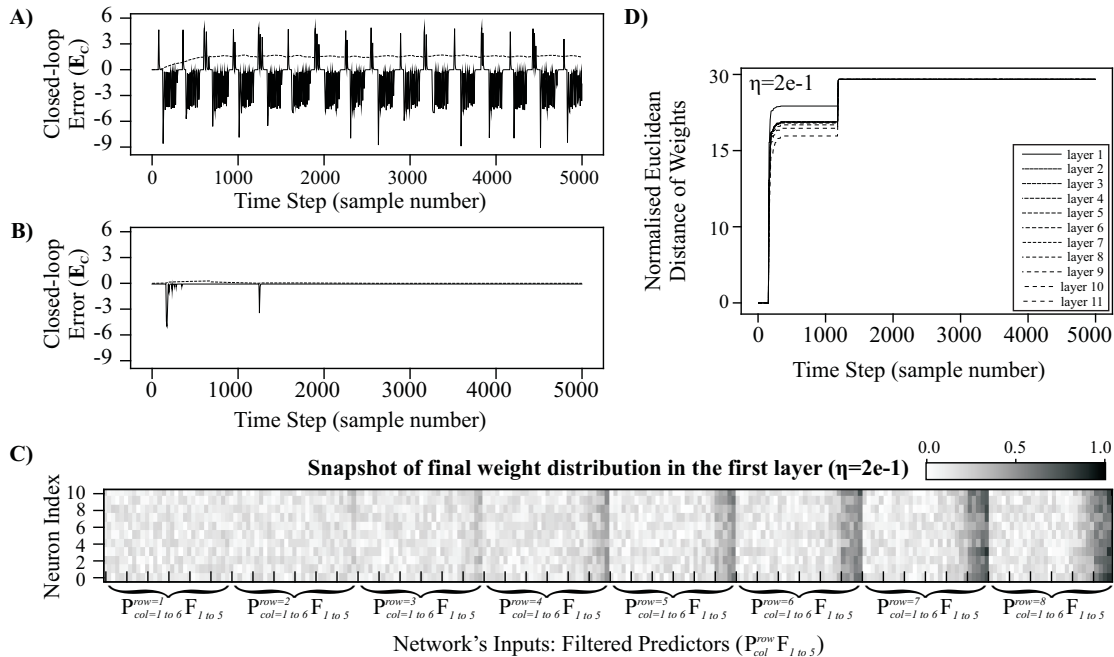


Figure 5: *Experimental results for learning rate of  $\eta = 2.10^{-1}$ : **A)** Shows the closed-loop error when robot navigates with reflex mechanism only. This sets a benchmark for evaluating the performance of the learning; note the high amplitude and persistence of this signal. **B)** Shows the closed-loop error when the learning mechanism governs the navigation of the robot. Note the significant reduction of the error signal compared to the reflex data showing fast learning. **C)** Shows a greyscale map of the weight distribution in the first layer after the learning has been completed. Note that the weight distribution closely follows the location of predictors to which they associate; with weights associated to outermost predictors having high values and weights associated to innermost predictors having small values to allow for abrupt and subtle steering of the robot respectively. This greyscale mapping is also illustrated in Fig. 2A. **D)** Shows normalised euclidean distance of the weights in each layer during learning.*

## 7 Discussion

In this paper we have presented a learning algorithm which creates a forward model of a reflex employing a multi layered network. Previous work in this area used shallow [Kulvicius et al., 2007], usually single layer networks to learn a forward model [Nakanishi and Schaal, 2004, Porr and Wörgötter, 2006] and it was not possible to employ deeper structures. On the other hand model free RL has been using more complex network structures such as deep learning by combining it with Q-learning where the network learns to estimate an expected reward [Guo et al., 2014, Bansal et al., 2016]. At first sight this looks like two competing approaches because they both use deep networks with error backpropagation. However, they serve different purposes as discussed in Dolan and Dayan [2013], Botvinick and Weinstein [2014] which lead to the idea of hierarchical RL where RL provides a prediction error for an actor which can then develop forward models.

Both, in deep RL [Guo et al., 2014] and in our algorithm we employ error backpropagation which is a mathematical trick where an error/cost function is expanded with the

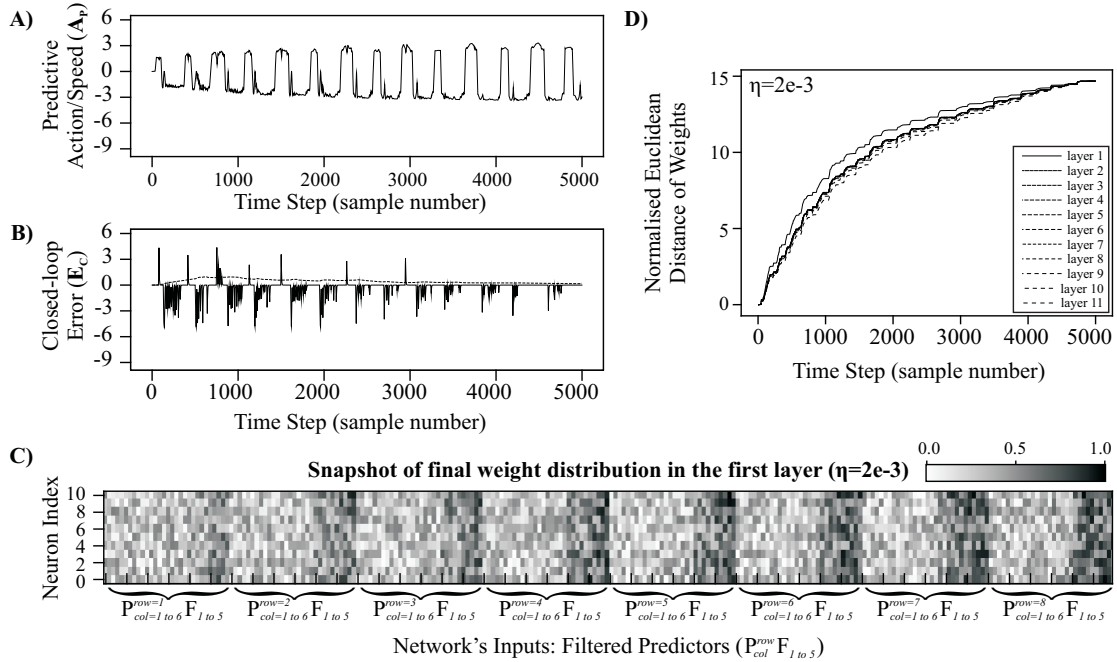


Figure 6: *Experimental results for learning rate of  $\eta = 2.10^{-3}$ : **A**) Shows the predictive action of the network  $A_P$ . This is the contribution of the learning to the steering of the robot is anticipation of a disturbance (turn in the road). Note that as the learning improves the amplitude of the steering increases and becomes more precise. **B**) Shows the closed-loop error when the learning mechanism governs the navigation of the robot. Note that the error is continuously reduced over time as the learning progresses. **C**) Shows a greyscale map of the weight distribution in the first layer after the learning is completed. Note that the weight distribution closely follows the location of predictors to which they associate, with weights associated to outermost predictors having high values and weights associated to innermost predictors having small values to allow for abrupt and subtle steering of the robot respectively. This greyscale mapping is also illustrated in Fig. 2A. **D**) Shows normalised euclidean distance of the weights in each layer during learning.*

help of partial derivatives [Rumelhart et al., 1986]. This approach is appropriate for open loop scenarios but for closed loop one needs to take into account the endless recursion caused by the closed loop. In order to solve this problem we have switched to the z-domain in which the recursion turns into simple algebra. A different approach has been taken by LSTM networks where the recursion is unrolled and backpropagation in time is used to calculate the weights [Hochreiter and Schmidhuber, 1997] which is done offline whereas in our algorithm this is done while the agent acts in its environment.

Deep learning is generally a slow learning algorithm and deep RL tends to be even slower because of the sparsity of the discrete rewards. On the other hand purely continuous or sampled continuous systems can be very fast because they have continuous error feedback so that in terms of behaviour nearly one shot learning can be achieved [Porr and Wörgötter, 2006]. However, this comes at the price namely that forward models are learned from simple reflex behaviours and no sophisticated planning can be achieved. For that reason it has been suggested to combine the model free deep RL

with model based learning to have a slow and a fast system [Botvinick et al., 2019].

Forward models play an important role in robotic and biological motor control [Wolpert and Kawato, 1998, Wolpert et al., 2001, Haruno et al., 2001, Nakanishi and Schaal, 2004] where forward models guarantee an optimal trajectory after learning and with our approach this offers opportunities to learn more complex forward models with the help of deep networks and then combine it with traditional Q-learning to planning those movements.

## References

Inter domain learning (IDL) source code. 10.5281/zenodo.3203391, 2019.

S. Bansal, A. K. Akametalu, F. J. Jiang, F. Laine, and C. J. Tomlin. Learning quadrotor dynamics using neural network for flight control. In *2016 IEEE 55th Conference on Decision and Control (CDC)*, pages 4653–4660, Dec 2016. doi: 10.1109/CDC.2016.7798978.

Mathew Botvinick, Sam Ritter, Jane X Wang, Zeb Kurth-Nelson, Charles Blundell, and Demis Hassabis. Reinforcement learning, fast and slow. *Trends in cognitive sciences*, 2019.

Matthew Botvinick and Ari Weinstein. Model-based hierarchical reinforcement learning and human action control. *Philosophical Transactions of the Royal Society B: Biological Sciences*, 369(1655):20130480, 2014. doi: 10.1098/rstb.2013.0480.

Ray J Dolan and Peter Dayan. Goals and habits in the brain. *Neuron*, 80(2):312–325, 2013.

Xiaoxiao Guo, Satinder Singh, Honglak Lee, Richard L Lewis, and Xiaoshi Wang. Deep learning for real-time atari game play using offline monte-carlo tree search planning. In Z. Ghahramani, M. Welling, C. Cortes, N. D. Lawrence, and K. Q. Weinberger, editors, *Advances in Neural Information Processing Systems 27*, pages 3338–3346. Curran Associates, Inc., 2014.

Masahiko Haruno, Daniel M. Wolpert, and Mitsuo Kawato. Mosaic model for sensorimotor learning and control. *Neural Computation*, 13:2201–2220, 2001.

Sepp Hochreiter and Jrgen Schmidhuber. Long short-term memory. *Neural Computation*, 9(8):1735–1780, 1997. doi: 10.1162/neco.1997.9.8.1735.

A. Harry Klopff. A drive-reinforcement model of single neuron function. In John S. Denker, editor, *Neural Networks for Computing: Snowbird, Utah*, volume 151 of *AIP conference proceedings*, New York, 1986. American Institute of Physics.

Tomas Kulvicius, Bernd Porr, and Florentin Wörgötter. Chained learning architectures in a simple closed-loop behavioural context. *Biological Cybernetics*, 97:363–378, 2007.

Jun Nakanishi and Stefan Schaal. Feedback error learning and nonlinear adaptive control. *Neural Networks*, 17(10):1453–1465, 2004.

- Charles L. Phillips. *Feedback control systems*. Prentice-Hall International (UK), London, 2000.
- Bernd Porr and Florentin Wörgötter. Strongly improved stability and faster convergence of temporal sequence learning by utilising input correlations only. *Neural Computation*, 18(6):1380–1412, 2006.
- David E. Rumelhart, Geoffrey E. Hinton, and Ronald J. Williams. Learning representations by back-propagating errors. *Nature*, page 533, 1986.
- R. S. Sutton and A. G. Barto. *Reinforcement Learning: An Introduction*. Bradford Books, MIT Press, Cambridge, MA, 2002 edition, 1998.
- P.F.M.J Verschure and A.C.C. Coolen. Adaptive fields: Distributed representations of classically conditioned associations. *Network*, 2:189–206, 1991.
- Christopher J.C.H Watkins and Peter Dayan. Q-learning. *Machine Learning*, 8:279–292, 1992.
- Daniel M. Wolpert, Zoubin Ghahramani, and J. Randall Flanagan. Perspectives and problems in motor learning. *TRENDS in Cognitive Sciences*, 5(11), 2001.
- D.M Wolpert and M. Kawato. Multiple paired forward and inverse models for motor control. *Neural Networks*, 11:1317–1329, 1998.